Available online at www.scholarsresearchlibrary.com

Scholars research library

Archives of Applied Science Research, 2011, 3 (5):514-525
(http://scholarsresearchlibrary.com/archive.html)

ISSN 0975-508X
CODEN (USA) AASRC9

Synthesis, dielectric, AC conductivity and non-linear optical studies of electrospun copper oxide nanofibers

G. Nixon Samuel Vijayakumar[a,b], M. Rathnakumari[b] , P.Sureshkumar[b*]

[a]Department of Physics, R.M.K.Engineering College, Kavaraipettai, India
[b]Materials Research Centre, Department of Physics, Velammal Engineering College, Chennai, Tamilnadu, India

---

ABSTRACT

Poly (Vinyl Alcohol) (PVA) / copper acetate sol prepared by sol-gel process was deposited on the collector by electrospinning and composite nanofibers were obtained. Calcining these composite fibers at 700^{o} C resulted in nanofibers of copper oxide (CuO) with diameters of 150 – 200 nm which was revealed by the Scanning Electron Microscope (SEM) and Atomic Force Microscope (AFM) images. The sample was characterized by Powder X-ray Diffraction (XRD) which established the presence of monoclinic copper oxide phase. Ultraviolet–Visible–near-Infrared Spectroscopy (UV–vis–NIR) was taken to obtain band gap value and it was calculated to be 2.5 eV. Energy Dispersive X-ray analysis (EDAX) confirmed the elements present in the sample. Dielectric properties and AC conductivity of the nanomaterial at different temperatures were studied with respect to frequency.

Keywords: Sol-gel process, Dielectric property, Electrospinning, Non-linear optic property, SEM.

INTRODUCTION

Metal oxide nanomaterials like copper oxide have shown massive significance in the fields of gas sensing, optoelectronics, catalysis, solar cells, etc due to their unique physical, thermal, chemical, optical, electrical, magnetic and mechanical properties. CuO is a semiconductor with narrow band gap suitable for potential applications [1-4]. Quite a lot of methods have been suggested for the synthesis of such materials including sol-gel process [5], ultrasound assisted method [6], hydrothermal synthesis [7], spray pyrolysis [8] and organochemical route [9].

Nanoscale materials in one dimension such as nano tubes, nanowires, nanorods, nanofibers, etc have fascinated recent researchers by their scientific and technological applications [10].

Nanofibers are used efficiently as gas sensors [11], electrodes [12], light emitters [13], super capacitors [14] and space-power providers [15] because of their large surface area per unit mass, smaller pore size and low basis weight. Nanocomposite materials are desirable due to their compliant nature in the design of fruitful electronic devices.

Electrospinning technique and sol – gel process are combined together to synthesize nanofibers. Some novel metal oxide fibers such as niobium oxide [16], zinc oxide [5], cerium oxide [17], palladium oxide [18] and NiO/ZnO composite [19] have been successfully synthesized by the electrospinning process. These fibers were calcined at high temperatures to obtain crystalline fibers. We have recently published a paper on the dielectric and non linear optical properties of ZnO/CuO nanocomposite fibers [20].

MATERIALS AND METHODS

1.1 Materials

Poly (vinyl alcohol) (M. W. = 1, 25, 000) and copper acetate extra pure were purchased from Merck and used without further refinement. Deionised water was used as solvent.

1.2 Preparation of PVA / copper acetate composite gel

30 g aqueous PVA solution (about 10 wt %) was prepared and stirred for 1 h. 2.4 g of copper acetate was dissolved in 20 mL of deionised water and slowly it was added to the already prepared aqueous PVA solution under stirring at 60˚ C for one hour. A viscous, clear sol solution of PVA / copper acetate was prepared by keeping in a water bath at 50 ˚ C under stirring for 6 h and later utilized in electrospinning.

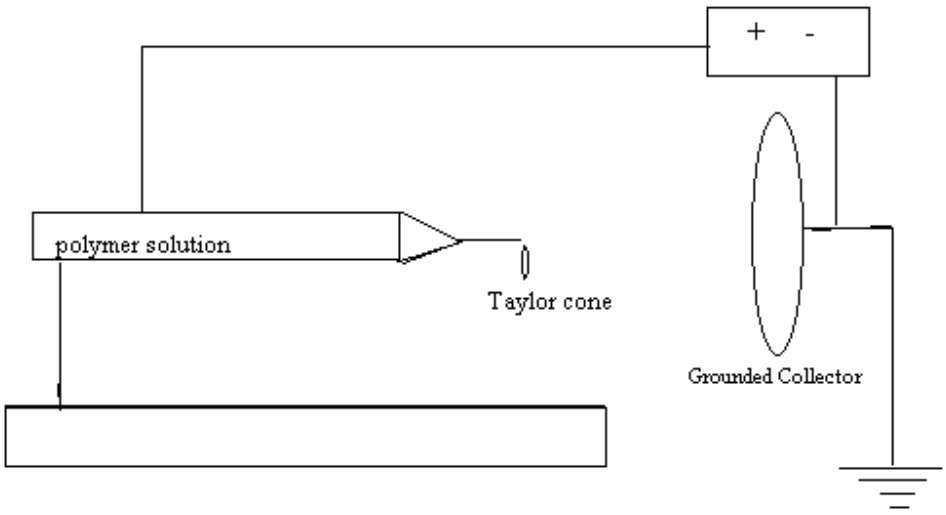

Fig.1 Electrospinning Setup

1.3 Preparation of nanofibers

The electrospinning apparatus is shown in Fig. 1. The viscous PVA/ copper acetate composite sol solution was taken in a 5 mL syringe. The hypodermic syringe needle was connected to the positive of the high voltage DC generator (10 to 40 kV) and the negative of the generator was connected to a grounded collector. A thin Al_2O_3 foil was placed on the collector opposite to the syringe needle at a distance of 12 cm. Upon applying a high voltage (13 kV) into the solution, a fluid jet was ejected from the syringe needle. Whenever the jet was accelerated towards the cathode, the solvent evaporated and a charged fiber was deposited on the Al_2O_3 foil fixed on the cathode. The formed fibers were dried for 10 h at 75˚ C under vacuum and then calcined at the rate of 240˚ C / h and remained 6 h at 700˚ C temperature.

The optimum values of the electrospinning parameters for the prepared PVA / copper acetate sol are given in Table.1. The sol was electrospun into nanofibers under the optimized conditions.

Table.1 Optimum values of electrospinning parameters

Electrospinning parameters	Optimized values
Applied voltage	16 kV
Distance between electrodes	14 cm
Size of the needle opening	25 G
Conductivity of the sol	15.6 mS/cm
Temperature of the sol	303 K
Viscosity of the sol	1.03 Pa.s
Calcining temperature	973 K
Time of calcining	6 h
Average diameter of fibers after calcining	125 nm

1.4 Characterization

Conductivity of the sol was measured by EQUIP-TRONICS model EQ-660A digital conductivity meter and viscosity of the sol was measured by Digital Viscometer. To observe the surface morphology and cross-section of the nanofibers, SEM images were captured using a JEOL GSM-5900 Scanning Electron Microscope. To determine the elemental composition, energy dispersive x-ray analysis (EDAX) was performed by using the same instrument. AFM images were also captured to validate the cylindrical morphology of the nanofibers by using AFM (NanoSurf Easy Scan2, Switzerland). The phase composition of the prepared samples were studied from the powder X – ray diffraction (XRD) patterns of the samples observed by a Rigaku D/max-A diffractometer fitted with CuKα radiation (λ=1.5406 A˚) at a scan speed of 0.01°/s at room temperature. The intensity data was recorded by continuous scan in 2θ/θ mode from 10° to 70°. UV spectrum was obtained by using VARIAN CARY 5E spectrophotometer. HIOKI 3532-50 LCR HITESTER meter was used to take the dielectric measurements with respect to frequency at different temperatures. From the non-woven mesh of the fibers, pellets of 0.43 mm thickness and 9.41 mm diameter were made by applying a pressure of 4 tonnes in a hand operated hydraulic press for performing the dielectric measurements. Kurtz–Perry powder technique was employed to test the second harmonic generation (SHG) efficiency of the sample.

RESULTS AND DISCUSSION

1.5 Scanning electron microscopy (SEM) and Atomic force microscopy (AFM)

The SEM images of PVA / copper acetate fibers and the fibers calcined at 700˚ C are shown in the Fig. 2(a) and 2(b).

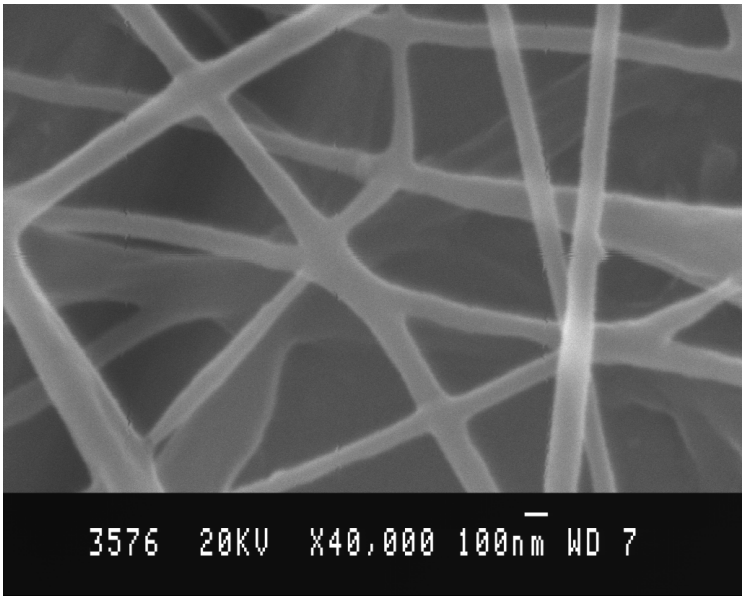

Fig.2(a) SEM image of Poly (Vinyl Alcohol) / copper acetate composite fibers

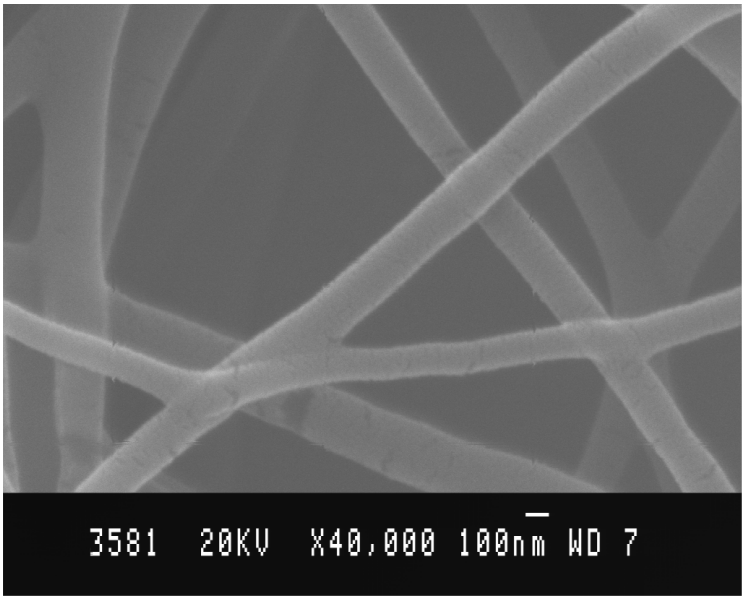

Fig.2(b) CuO nanofibers after calcining at 700° C

It could be clearly seen that the smooth fibers with diameters of 150 to 200 nm were obtained only by calcining the PVA / copper acetate fibers at 700˚ C.

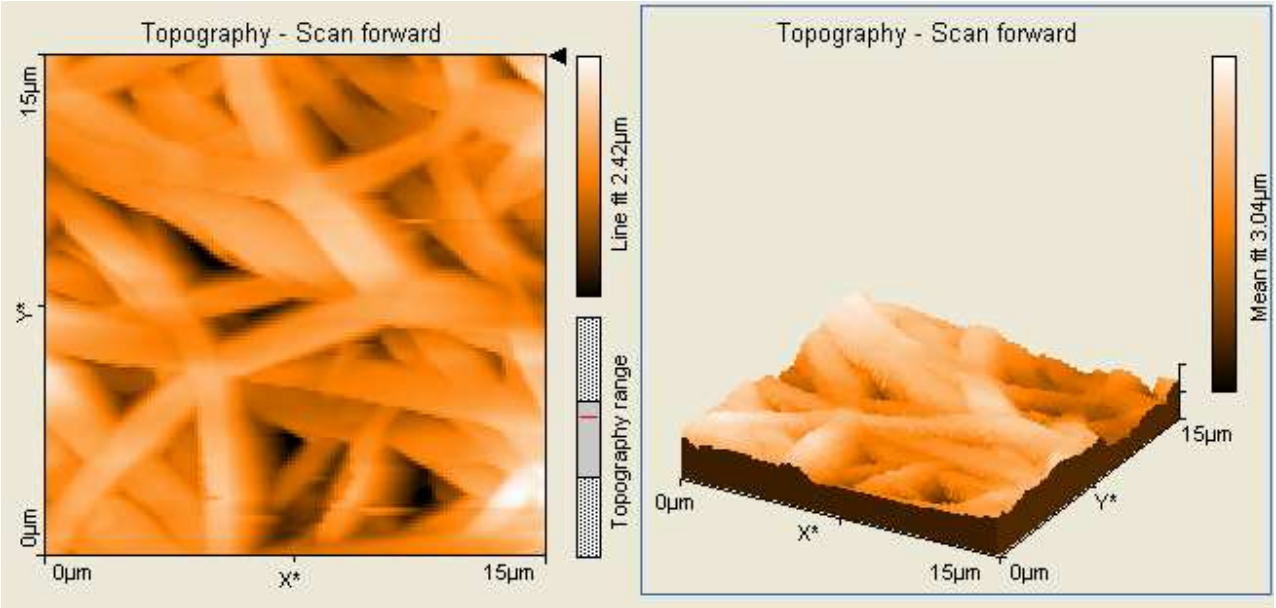

Fig.3 AFM image of Poly (Vinyl Alcohol) / copper acetate composite fibers

Atomic Force Microscopy was used to confirm the cylindrical morphology of the electrospun fibers. Fig.3 represents the AFM image of PVA / copper acetate composite fibers. From Fig.3, it is obvious to observe the cylindrical morphology of the PVA / copper acetate composite fibers. The fibers are uniformly distributed on the collector screen.

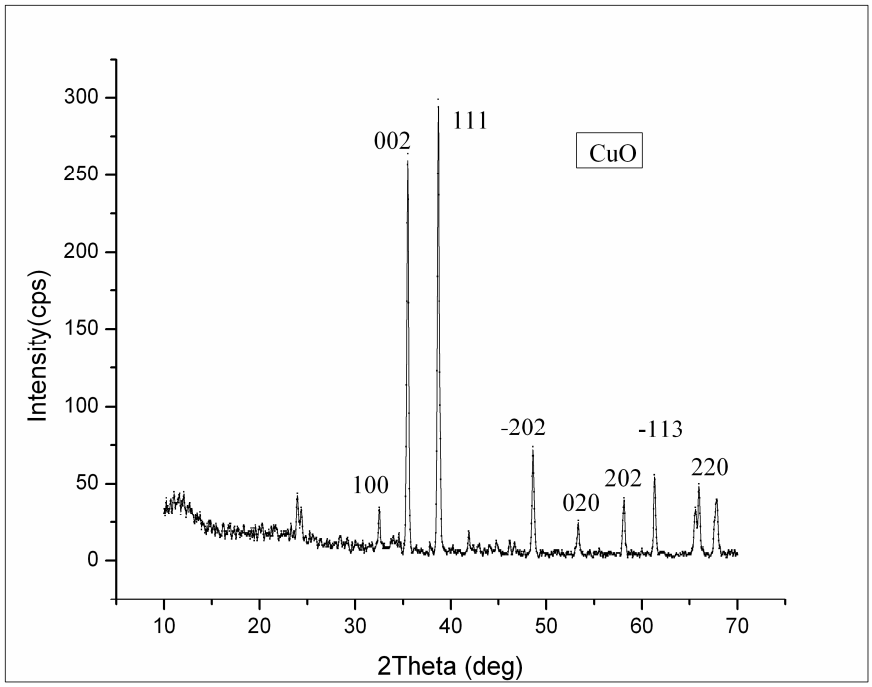

Fig.4 Powder XRD spectrum of calcined CuO nanofibers

1.6 Powder x-ray diffraction

Fig.4 gives the XRD curves for calcined fiber samples. After calcining at 700˚ C, the semi-crystalline peak for PVA around 2θ = 20^{o} corresponding to (101) plane [21] disappeared. XRD spectra of the fibers after calcinations at 700˚ C showed peaks at 32.3˚(110), 35.4˚(002), 38.5˚(111), 48.5˚ (202), 53.1˚(020), 57.9˚ (202), 61.1˚(113) and 67.5˚(220) corresponding to CuO agreed very well with the literature [3]. It corresponds to monoclinic copper oxide phases which are in very good agreement with reported values in the literature JCPDS – 5 – 0661

3.3 EDAX analysis

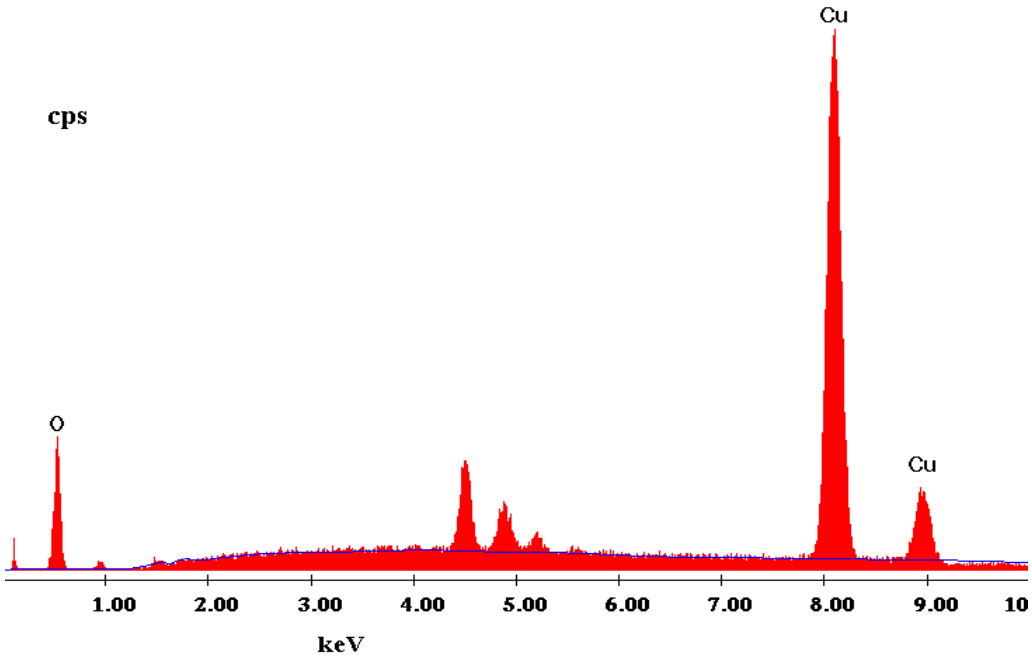

Fig.5 EDAX spectrum of the calcined CuO nanofibers

Fig.5 gives the EDAX spectrum of the calcined CuO nanofibers at 700^{o} C. It confirms the presence of the elements in CuO. From the EDAX measurements, it was obtained that Cu and O are present in the weight percentages of 92.33 and 7.67 respectively.

3.4 Optical absorption studies

The optical absorption spectrum of CuO nanofiber was recorded in the wavelength region from 200 to 2000 nm and is shown in Fig.6. The UV absorption edge for the CuO nanofiber was observed to be around 260 nm. The dependence of optical absorption coefficient with the photon energy helps to study the band structure and the type of transition of electrons.

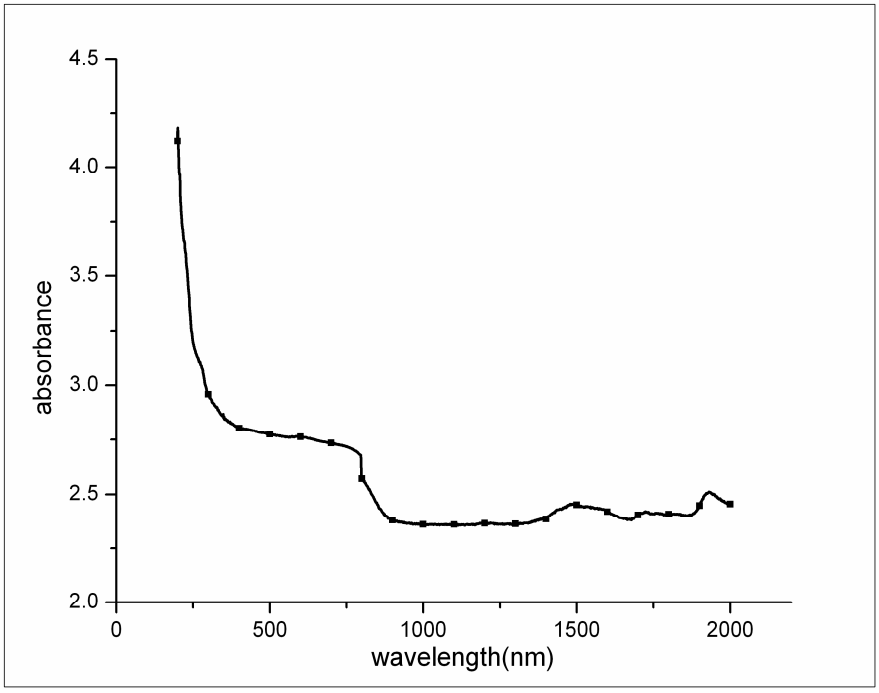

Fig.6 UV spectrum of the CuO nanomaterial

For the direct band gap material, the CuO nanofiber under study has an absorption coefficient (α) obeys the subsequent relation for high photon energies (hν) according to Tauc expression [22]

$$\alpha = \frac{A(h\nu - E_g)^{1/2}}{h\nu}$$

Where E_g is the optical band gap of the nanofiber and A is a constant. The plot of variation of $(\alpha h\nu)^2$ versus hν is shown in the Fig.7. Band gap E_g is evaluated by the extrapolation of the linear part [23]. The band gap is calculated to be 2.5 eV. The comparison of bandgap energy of CuO nanomaterial with different forms is given in Table.2.

Table. 2 Comparison of band gap energy

Name of the material	Band gap energy in eV
CuO nanofiber	2.5
CuO thin film by reactive magnetron sputtering	2.4 [24]
CuO thin film by activated reactive evaporation	2.1 [25]
ZnO/CuO nanofiber	3.1 [20]

3.5 Dielectric Property

Fig. 8 shows the variation of dielectric constant (ε_r) with respect to frequency for the nanomaterial at various temperatures of 308, 323 and 343 K. Using the expression, the dielectric constant (ε_r) of the nano sample was calculated. Where C is the capacitance, d is the thickness,

A is the surface area of the sample and ε_0 is the absolute permittivity of free space (8.854 × 10^{-12} F/m).

$$\varepsilon_r = \frac{Cd}{\varepsilon_0 A}$$

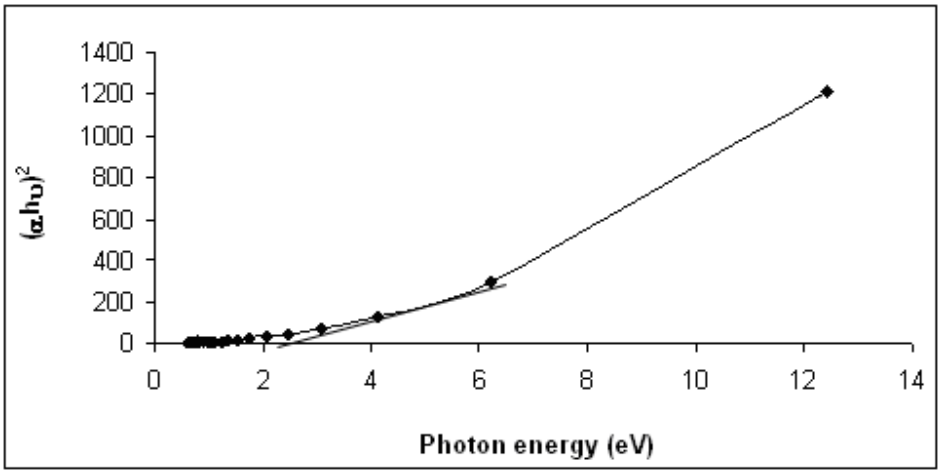

Fig.7 Plot of variation of $(\alpha h\nu)^2$ vs hν

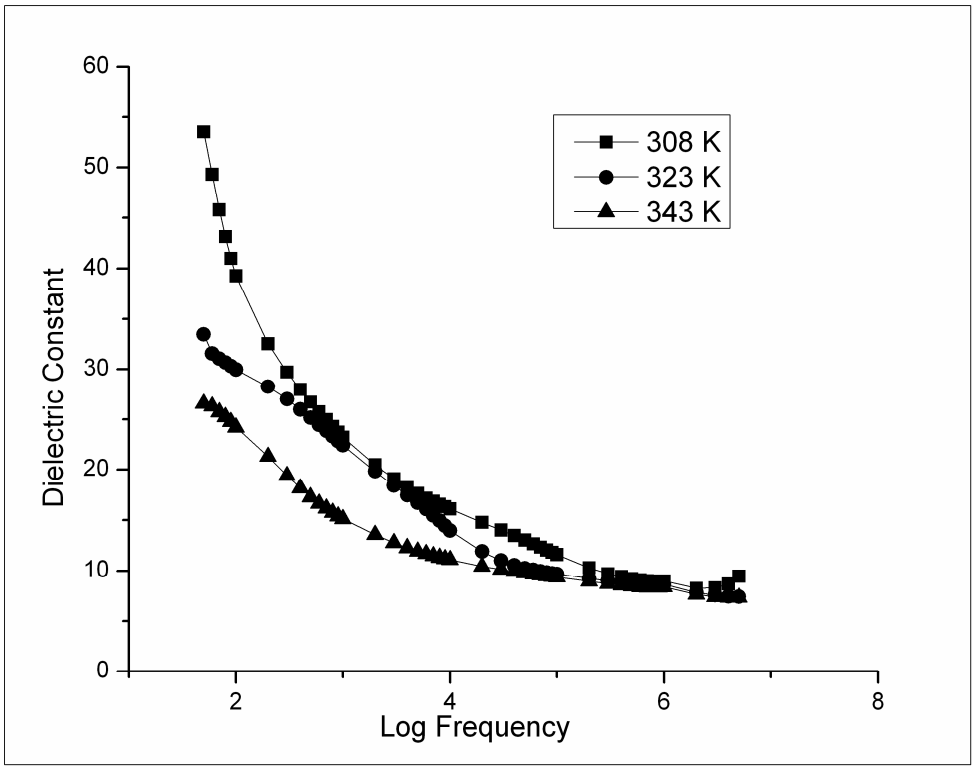

Fig.8 Frequency dependence of dielectric constant

From the graph, it is seen clearly that the dielectric constant has high values in the low frequency regions for the nano material. This is due to the existence of various types of polarization mechanisms like electronic, ionic, orientation and space charge polarization [26]. This may lead to large values of dielectric constant at low frequencies. Due to the application of an electric field the space charges are moved and dipole moments are created. This is called as space charge polarization. In addition to this, these dipole moments are rotated by the field applied resulting in rotation polarization which is also contributing to the high values. Whenever there is an increase in the temperature, more dipoles are created and the value increases [27]. In the high frequency region, before the field reversal occur the charge carriers may have started to move and dielectric constant falls to a small value.

Fig. 9 shows the variation of dielectric loss with respect to the frequency for calcined material at various temperatures of 308, 323 and 343 K. It is quite obvious that for all temperatures the dielectric loss decreases with increase in the frequency which follows a similar trend as the decrease in the dielectric constant . This shows that the dielectric loss is strongly reliant on the frequency of the applied field. At high frequencies, the very low dielectric loss exhibited may be related with the purity of the nanomaterial, having negligible defects with good optical quality which could be useful in the design of optical devices [28].

3.6 A. C. conductivity studies

The a.c.conductivity of the sample can be determined by using the relation $\sigma_{a.c} = 2\pi\varepsilon_0\varepsilon_r f \tan\delta$. where ε_0 is permittivity in free space, ε_r is dielectric constant, f is the frequency and tan δ is the loss factor. The a.c.electrical conductivity of the nanomaterial as a function of frequency and temperature is shown in Fig.10. There is a small increase in the electrical conductivity of the nano material at the low frequency region, for an increase in frequency. This pattern is the same for all temperatures. But, at high frequencies especially in the MHz region, there is an abrupt increase in the conductivity and it is enormous at high temperatures. The high ac conductivity high temperatures could be attributed to small polaron hopping [29]. The increase in conductivity with temperature may be explained based on the assumption that within the bulk, the oxygen vacancies due to the loss of oxygen, are usually created during increase in temperature and the charge compensation, which would leave behind free electrons. In metal oxides, electrical conduction occurs through strong coupling between phonons and electrons with the creation of polarons.

3.7 Second harmonic generation efficiency (SHG)

The CuO nanomaterial was tested for its second harmonic generation efficiency with reference to KDP by using the Kurtz-Perry powder technique. In the experiment, the laser powder output was kept constant throughout the experiment. The sample was illuminated by using an Nd:YAG laser of wavelength 1064 nm which resulted in an output of green wavelength of 532 nm. Thus the doubling of input frequency was confirmed. The output power of the CuO nanomaterial is found to be 0.75 times that of KDP.

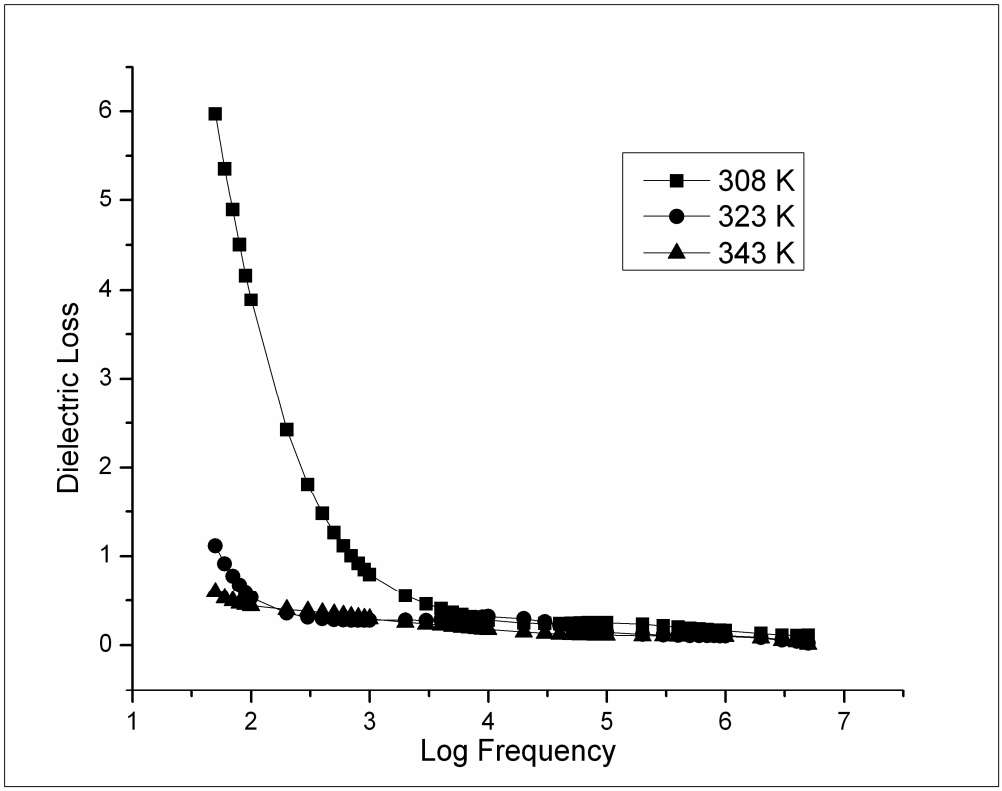

Fig.9 Frequency dependence of dielectric loss

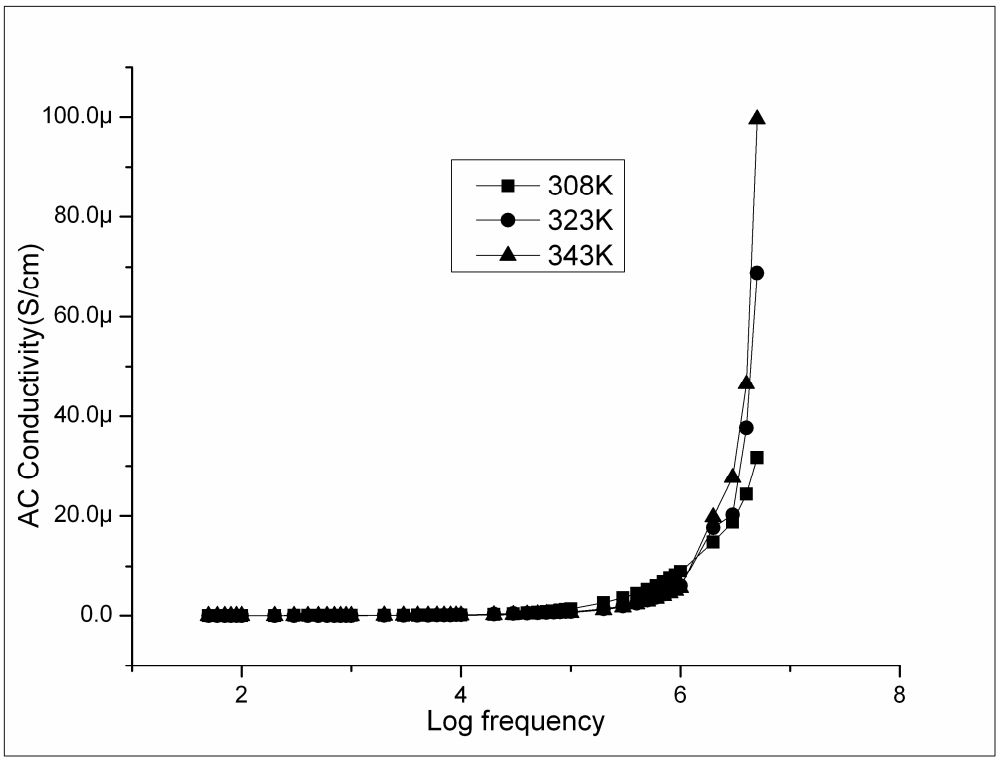

Fig.10 Frequency dependence of AC conductivity

Table.3 Comparison of SHG efficiency of CuO with other materials

Compound name	SHG efficiency compared with KDP	Reference
ZnO nanofiber	0.67 times	Present work
CuO nanofiber	0.75 times	Present work
Urea	7.50 times	Present work
ZnO/CuO nanofiber	11.10 times	[20]

CONCLUSION

Copper oxide nanofibers were synthesized using PVA / copper acetate precursor and through successive calcination treatment. The diameters were found to be between 150 – 200 nm .The fibers were characterized by SEM, AFM, XRD, UV and EDAX respectively. Smaller diameter fibers could be synthesized by varying the sol-gel parameters or modifying the electrospinning process variables. This would be a hopeful approach for the large scale fabrication of one dimensional copper oxide nano fibers for fruitful realistic applications.

Acknowledgement
The authors wish to express their thanks to the IISc, Bangalore for the NLO test, EDAX and SEM images, Loyola college, Chennai for the dielectric studies and Department of Nuclear Physics, Madras University for the powder X-ray diffraction studies.

REFERENCES

[1] Jenna Pike, Siu-Wai Chan , Feng Zhang , Xianqin Wang and Jonathan Hanson: *Appl.Catal. A: Gen.*, **2006**, 303, 273-277.
[2] C T Hsieh, J M Chen , H H Lin, and H C Shih, *Appl. Phys. Lett.*, **2003**, 83, 3383-3385.
[3] M A Dar, Q Ahsanulhaq , Y S Kim, J M Sohn, W B Kim, and H S Shin, *Appl. Sur. Sci.*, **2009**, 255, 6279-6284
[4] Oleg A. Yeshchenko , Igor M. Dmitruk, Andriy M. Dmytruk and Alexandr A. Alexeenko: *Mater. Sci. and Eng.* B, **2007**, 137, 247-254.
[5] R Siddheswaran , R Sankar , M Ramesh Babu , M Rathnakumari , R Jayavel , P Murugakoothan , and P Sureshkumar , *Cryst. Res. Technol*., **2006**, 41, 446 – 449.
[6] A I Isayev, Rishi Kumar, Todd M. Lewis, *Polym* , **2009**, 50, 250-260.
[7] Nasser AM. Barakat, Soo Jin Park, Myung Seob Khil and Hak Yong Kim: *Mater. Sci. and Eng: B,* **2009**, 162, 205-208.
[8] M R Islam and J Podder *J, Cryst. Res. Technol*., **2009**, 44, 286-292.

[9] Yong Jae Kwon, Kyoung Hun Kim, Chang Sung Lim and Kwang Bo Shim: *J. Ceram. Process. Res.*, **2002**, 3(3), 146-149.
[10] Ioannis S. Chronakis *: J.Mater.Process.Technol*., **2005**, 167, 283-293.
[11] Bin Ding, Michiyo Yamazaki and Seimei Shiratori: *Sens and Actuators* B, **2005** 106,477-483.
[12] Mi Yeon Song, Do Kyun Kim, Seong Mu Jo and Dong Young Kim: *Syn. Metals*, **2005**, 155, 635 -638.

[13] V Tomer , R Teye-Mensah , J C Tokash, N Stojilovic, W Kataphinan , E A Evans , C G Chase, R D Ramsier , D J Smith, and D H Reneker, *Sol. Energy Mater. & Sol. Cells*, **2005**, 85,: 477-488.
[14] Chan Kim, Yeong-Og Choi, Wan-Jin Lee and Kap-Seung Yang: *Electrochimica Acta*, **2004**, 50, 883-887.
[15] G Zhang, W Kataphinan , R Teye-Mensah, P Katta , L Khatri , E A Evans , G G Chase, R D Ramsier , and D H Reneker , *Mat. Sci. Eng., B.*, **2005**, 116, 353 -358.
[16] P Viswanathamurthi , N Bhattarai , H Y Kim, D R Lee, S R Kim, M A Morris, *Chem. Phys.Letters*, **2003**, 37, 79-84.
[17] Qizheng Cui, Xiangting Dong, Jinxian Wang and Mei Li: J.Rare Earths, **2008**, 26,664-669.
[18] P Viswanathamurthi, N Bhattarai , H Y Kim, D I Cha ,and D RLee, *Mater. Letters*, **2004** , 58, 3368-3372.
[19] Changlu Shao, Xinghua Yang, Hongyu Guan, Yichun Liu and Jian Gong: *Inorg. Chem Commun*, **2004**, 7, 625-627.
[20] G Nixon Samuel Vijayakumar , S Devashankar , M Rathnakumari , P Sureshkumar **2010**, 507, 225-229.
[21] Y Nishio, and R S J Manley., *Macromolecules*, **1988**, 21, 1270-1277.
[22] G P Joshi, N S Saxena, R Mangal , A Mishra , and T P Sharma , *Bull. Mater. Sci*., **2003**, 26(4), 387-389.
[23] A K Chawla, D Kaur , and R Chandra , *Opt. Mater*., **2007**, 29,:995-998.
[24] A.A Ogwu, T.H Darma, E Bouquerel , *J of Achievements in Mat. and Manufacturing Engg* , **2007**, 24(1), 172-177
[25] B Balamurugan , B R Mehta, *Thin Solid Films* **2001**,396, 90-96.
[26] C M Mo, L Zhang , and G Wang , *Nanostruct. Mater*. **1995**, 6, 823-826.
[27] A Boomadevi A ,H P Mittal, and R Dhansekaran R., *J. Cryst. Growth*, **2004**, 261, 55-62.
[28] P.M Ushasree, R Jayavel and .P Ramasamy , *Mater. Chem. Phys*, **1999**, 61, 270- 274.
[29] I G Austin, N F Mott, *Adv. Phys*., **1969**, 18, 41-102.